Mechanical Properties and Durability of High-Strength Concrete for Prestressed Bridge Girders

ALIREZA MOKHTARZADEH, ROXANNE KRIESEL, CATHERINE FRENCH, AND MARK SNYDER

Results from a comprehensive laboratory investigation on the application of high-strength concrete to the production of precast/prestressed bridge girders are presented. The portion of the laboratory investigation described consisted of producing high-strength concrete with a variety of cementitious materials (portland cement, silica fume, and fly ash) in different proportions and made with five different types of coarse aggregate. Some specimens were moist cured in saturated-limewater at 23°C; others were heat cured in an environmental chamber at 65°C to simulate the accelerated curing technique typically used by precast/prestressed plants. The hardened concrete specimens were tested for compressive strength, modulus of elasticity, tensile strength, modulus of rupture, shrinkage, creep, absorption potential (as an indirect indicator of permeability), and freeze-thaw durability.

An extensive investigation is under way at the University of Minnesota to study the application of high-strength concrete to prestressed bridge girder production. High-strength concrete is defined as concrete with a 28-day compressive strength in excess of 41 MPa. The objective of the study is to obtain information on production techniques, mechanical properties, and durability of high-strength concrete in general and to provide recommendations for using these concretes in manufacturing precast/prestressed bridge girders. Test variables include total amount and composition of cementitious material [portland cement, fly ash (FA), and silica fume (SF)], type and brand of cement, type of silica fume (dry-densified and slurry), type and brand of high-range water-reducing admixture, coarse-to-fine aggregate ratio, type of aggregate, aggregate gradation, maximum aggregate size, and curing. Tests are being conducted to determine the effects of these variables on changes in compressive strength and modulus of elasticity over time, splitting tensile strength, modulus of rupture, creep, shrinkage, absorption potential [as an indirect indicator of permeability (*1*)], and freeze-thaw durability. Also being investigated are the effects of test parameters such as mold size, mold material, and end condition. Nearly 7,000 specimens have been cast from approximately 150 mixes over a period of 3 years (*2,3*).

This paper presents results from a portion of the study (20 mixes) for which total cementitious material content, water-to-cementitious material ratio, and coarse-to-fine aggregate ratio were held constant at 445 kg/m^3, 0.30, and 1.5, respectively. Four different cementitious material combinations were investigated: reference mix (portland cement only) and three comparison mixes containing 20 percent FA, 7.5 percent SF, and a combination of 20 percent FA with 7.5 percent SF. For the three comparison mixes, the fly ash and silica fume were incorporated as replacements for portland cement on an equal weight basis. Five different types of locally obtained coarse aggregates were used in this phase of the investigation: round gravel (RG), partially crushed gravel (PCG), crushed granite (GR), and a high-absorption (LS–H) and a low-absorption (LS–L) crushed limestone. From each concrete batch, both heat- and moist-cured specimens were investigated.

Department of Civil Engineering , University of Minnesota, 122 Civil Engineering Building, 500 Pillsbury Drive, S.E., Minneapolis, Minn. 55455–0220.

MATERIALS

The cementitious material comprised low-alkali ASTM C150 Type III portland cement, ASTM C618 Class C fly ash, and silica fume slurry.

All the aggregates were obtained from local sources and washed in the laboratory. The coarse aggregates had a nominal maximum particle size of 13 mm. The natural coarse sand used in all mixes had a fineness modulus of 2.80. According to Minnesota Department of Transportation specifications, the maximum allowable absorption capacity for Class B aggregates (crushed quarry or mine rock) is 1.7 percent to ensure durable performance of concrete superstructures (*4*). Absorption capacities of the aggregates used in the study were 0.50 percent for the fine aggregate, 1.11 percent for the RG, 1.39 percent for the PCG, 1.00 percent for the granite, 2.05 percent for the LS–H (used in the reference and 7.5 percent silica fume mixes), 2.97 percent for the LS–H (used in the 20 percent fly ash and combination of 20 percent FA with 7.5 percent SF mixes), and 1.50 percent for the LS–L. The reason for listing two absorption capacities for the high-absorption limestone is that the aggregate was obtained at two different times from the same source.

A modified naphthalene sulfonate high-range water-reducer (superplasticizer) was used in varying quantities (13 to 23 mL/kg of cement) to attain a target slump of 100 to 150 mm. No air-entraining agents were used in the mixes, in conformance with typical precast girder production.

The moisture content of the aggregates and the water content of the SF slurry and superplasticizer were considered in proportioning the mix water. The mix proportions per cubic meter of concrete, as batched, are given in Table 1.

FABRICATION AND CURING PROCEDURES

For each mix investigated, all specimens were cast from a single batch. The mixing and curing was conducted in the Structural Labo-

TABLE 1 As-Batched Mix Proportions per Cubic Yard of Concrete

Mix	Coarse Aggr* (kg)	Fine Aggr* (kg)	Cement (kg)	Fly Ash (kg)	Silica Fume Slurry+ (kg)	Water∇ (kg)	HRWRΔ (g)
RG	1120	747	445	0	0	129	5569
RG w/FA	1112	742	356	89	0	129	5569
RG w/SF	1110	740	412	0	70	95	5569
RG w/FA&SF	1104	736	323	89	70	95	5569
PCG	1139	760	445	0	0	129	5569
PCG w/FA	1133	755	356	89	0	129	5569
PCG w/SF	1130	753	412	0	70	95	5569
PCG w/FA&SF	1124	749	323	89	70	95	5569
GR	1125	749	445	0	0	129	5569
GR w/FA	1117	746	356	89	0	129	5569
GR w/SF	1116	744	412	0	70	95	5569
GR w/FA&SF	1109	739	323	89	70	95	5569
LS-H	1147	765	445	0	0	129	5569
LS-H w/FA	1139	760	356	89	0	129	5569
LS-H w/SF	1138	759	412	0	70	95	5569
LS-H w/FA&SF	1130	753	323	89	70	95	5569
LS-L	1142	761	445	0	0	129	5569
LS-L w/FA	1135	756	356	89	0	129	5569
LS-L w/SF	1133	755	412	0	70	95	5569
LS-L w/FA&SF	1126	751	323	89	70	95	5569

* Values listed are for SSD moisture condition. Water was proportioned to compensate for actual moisture content of aggregates at time of mixing.
+ Silica Fume Slurry includes water weight (Solids: 659 kg/m^3 ; Water: 683 kg/m^3).
∇Water weight corresponding to SSD aggregate condition, adjusted for the amount of water in silica fume slurry and HRWR.
Δ Nominal amount of HRWR which was then adjusted (increased or decreased) during the mixing process to achieve the desired slump range of 100 to 150 mm.

ratory at the University of Minnesota. A 0.3-m^3 fixed-drum mixer powered by an electric motor was used to mix all of the concrete batches. Specimens cast from each mix included thirty-eight 100 × 200 mm and six 150 × 300 mm cylinders for compression tests (compressive strength and modulus of elasticity tests), three 150 × 300 mm cylinders for splitting tensile strength tests, four 150 × 150 × 610 mm beams for modulus of rupture tests, two 100 × 250 mm cylinders for shrinkage tests, and two 100 × 200 mm cylinders for absorption potential tests. Two 100 × 250 mm cylinders were cast from 14 of the mixes for creep studies. Four beams 76 × 102 × 406 mm were cast from 17 of the mixes for freeze-thaw durability testing. These quantities reflect that at least two duplicate specimens were fabricated to establish every test data point by averaging the results.

Mixing

Following evaluation of a few trial batches, the standard laboratory mixing and batching procedures recommended by ASTM C192 were modified slightly to allow an easy and uniform production technique. The mixing procedure followed these steps:

1. Spray interior of mixer with water. Empty the mixer and drain it.
2. Load the mixer with all coarse aggregate and half of the mixing water. Mix for ½ min.
3. Stop the mixer and allow the coarse aggregate to soak in the water for 10 min.
4. Turn on the mixer and add sand, cementitious material, remaining water, and high-range water-reducer. Mix for 5 min.
5. Stop the mixer for 1 min. Evaluate the workability. Add additional high-range water-reducer (up to a total of 23 mL/kg of cement), if needed.
6. Turn on the mixer for an additional 3 min.
7. Perform a final slump test and discharge the concrete into a clean, moist, metal bin and cast the specimens.

For each mix, slump and air contents were measured according to ASTM C143 and C173 (volumetric method) procedures, respectively. Results are given in Table 2 along with the 28-day compressive strengths of the heat- and moist-cured 100 × 200 mm specimens.

Casting and Curing

One day before mixing, the insides of all molds were lightly oiled with form coating oil. Molds were filled and manually rodded in accordance with the provisions of ASTM C192. All high-strength concrete specimens were cast in plastic molds except for the flexural modulus and freeze-thaw beams, which were cast in heavy-gauge reusable steel molds.

A 1460 L curing tank equipped with a thermostatically controlled electric heater was used to moist-cure concrete specimens. The specimens to be moist-cured were placed into the 23°C saturated-limewater bath immediately after casting. To avoid damage to the

TABLE 2 Air Contents, Slumps, and 28-Day Compressive Strengths

Mix	air content (%)	slump (mm)	f'c, heat-cured (MPa)	f'c, moist-cured for 7 days (MPa)	f'c, moist-cured for 28 days (MPa)
RG	1.5	127	77	98	91
RG w/FA	2.5	140	75	91	82
RG w/SF	1.5	70**	89	105	100
RG w/FA&SF	1.5	140	79	103	102
PCG	1.5	13*	89	111	104
PCG w/FA	2.0	89**	86	104	104
PCG w/SF	1.5	89**	99	113	108
PCG w/FA&SF	2.0	76**	91	114	110
GR	1.5	44*	87	99	98
GR w/FA	1.5	102	81	99	98
GR w/SF	1.5	NR	97	120	115
GR w/FA&SF	1.0	102	90	104	111
LS-H	1.5	152	104	118	114
LS-H w/FA	1.0	114	86	98	98
LS-H w/SF	NR	102	115	116	118
LS-H w/FA&SF	1.5	152	96	109	107
LS-L	1.5	38*	112	120	111
LS-L w/FA	1.0	102	98	101	103
LS-L w/SF	2.0	114	113	127	121
LS-L w/FA&SF	1.0	NR	111	124	110

*It was not possible to achieve the desired slump range of 100 to 150 mm without exceeding the maximum superplasticizer dosage of 23 ml per kilogram of cement (12282 g/m^3 of concrete).
NR Indicates measurement not recorded.
**For these mixes, adequate workability was achieved without meeting target slump range of 100 to 150 mm.

young specimens, molds were stripped after 48 hr (instead of 24 ± 8 hr, as specified by ASTM C192). The specimens were immediately returned to the saturated-limewater bath where they remained until testing, except the freeze-thaw beams, which were moist cured for 7 days.

To simulate the accelerated heat-curing process typical of precast/prestressed concrete manufacturers, an electronically controlled environmental chamber was used. The temperature in the chamber was varied according to the following procedure: 3 hr at room temperature (preset period after casting), temperature increased to 65°C over the next 2.5 hr, temperature held constant for 12 hr, and specimens returned to room temperature over 2 hr. To prevent loss of moisture from the fresh concrete, the surface of each heat-cured specimen was covered immediately after casting with a piece of plastic wrap held in place by a rubber band. The heat-cured specimen molds were stripped after 24 hr. These specimens were then stored in air in the laboratory until testing.

EXPERIMENTAL PROGRAM TO INVESTIGATE MECHANICAL PROPERTIES

All compression tests, splitting tensile strength tests, and modulus of rupture tests were conducted using an MTS Model 810 Material Testing System. The system has a dual capacity of 534 or 2,670 kN (tension or compression) and can be programmed to operate in either load or displacement control modes. For compression tests, the load was continuously applied to the specimens by moving the top spherical bearing block at a rate of 1.3 mm/min (displacement control mode).

The splitting tensile strength tests and flexural modulus tests were conducted under the load control mode with the 534 kN capacity of the testing machine selected. Specimens were loaded at a rate of 75.5 kN/min and 8 kN/min for splitting tensile strength and modulus of rupture tests, respectively. These loading rates corresponded to a stress increase of 1.03 MPa/min. The ASTM C496 (specification for

splitting tensile strength test) and ASTM C78 (specification for third-point loading flexural strength test) specified ranges for loading rates are 0.69 to 1.38 MPa/min and 0.86 to 1.21 MPa/min, respectively.

An aluminum compressometer, similar in principle to conventional compressometers used for standard cylinders, was built to measure Young's modulus of elasticity for 100 × 200 mm cylinders. A linear variable differential transformer (LVDT) with a maximum range of ±0.254 mm was mounted on this device to measure the sum of deformations of two diametrically opposite gauge lines. The gauge length for the axial deformation measurements was 100 mm. A conventional compressometer with a gauge length of 200 mm, equipped with a dial gauge, was used to measure Young's modulus of elasticity for the 150 × 300 mm cylinders. The 100 × 200 mm and 150 × 300 mm test cylinders were preloaded to 67 kN and 134 kN, respectively, and unloaded before testing for Young's modulus of elasticity. This initial loading and unloading was performed to ensure proper seating of the fixture on the test specimen.

The results of mechanical tests of compression strength and Young's modulus of elasticity changes with respect to time, splitting tensile strength, and modulus of rupture follow. Tests to investigate creep and shrinkage are still in progress.

Compression Tests

In this portion of the study, compression tests were conducted on 100 × 200 mm cylinders at different ages to study strength-time and elastic modulus-time relationships. For heat-cured specimens, tests were conducted at 1, 28, 182, and 365 days. Moist-cured specimens were tested at 28, 182, and 365 days (results are reported for data available up to 182 days). Compression tests on companion 150 × 300 mm cylinders were also conducted (at 1 and 28 days for heat-cured and 28 days for moist-cured specimens) to study size effects. All compression test specimens were capped using a high-strength sulfur-based capping compound.

Compressive Strength Change with Time

Table 3 summarizes the ranges of compressive strengths obtained for all mixes in this part of the study. Also shown in Table 3 are ratios of 1-day and 182-day strengths relative to 28-day strengths. These data indicate that the heat-cured specimens did not gain much compressive strength after 28 days. However, on average, 182-day-old continuously moist-cured specimens achieved compressive strengths that averaged approximately 10 percent greater than those measured at 28 days.

The effect of curing on strength gain over time for the LS–H reference mix is shown in Figure 1. In addition to the data described in this portion of the study (which are represented by filled symbols), additional data are included from the main body of tests (lines). The lines shown in the figure represent data obtained from identical mixes (except aggregate gradation) tested at more frequent intervals (1, 14, 28, 56, and 182 days). At early ages, the heat-cured specimens developed higher strengths (which is why heat-curing is used in precasting operations with short turnaround times on casting beds). At later ages (20 to 60 days), the strengths of the moist-cured specimens catch up with and then surpass those of the heat-cured specimens. This can be attributed to the continued hydration of cement in the moist-cured specimens and the reduced rate of hydration in the heat-cured specimens during the laboratory storage portion of their curing.

Figure 2 shows the effect of aggregate type on strength gain. In comparing the compressive strength of concrete made with crushed limestone (LS–H and LS–L) versus RG, the concrete made with limestone aggregates achieved higher compressive strengths. Crushed limestone particles showed a very strong bond with cement paste, and the plane of fracture in the limestone concrete crossed through many coarse aggregate particles. In contrast, the smooth surface of RG particles resulted in a relatively poor bond with cement paste, and the plane of fracture passed around all but the smaller coarse aggregate particles. Compressive strengths of the mixes using GR and PCG were between those of the limestone and

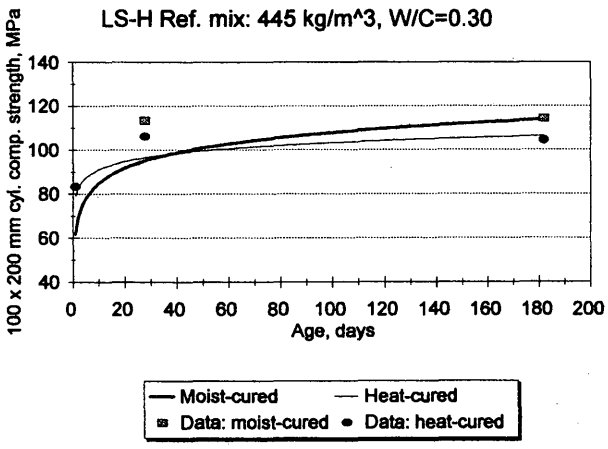

FIGURE 1 Effect of curing on strength gain with time.

TABLE 3 Compressive Strength Change with Time

	Heat-Cured	Moist-Cured
1-day Compressive Strength, MPa	44 - 101	-
28-day Compressive Strength, MPa	58 - 116	70 - 119
182-day Compressive Strength, MPa	63 - 117	87 - 122
Ratio of 1-day to 28-day Strength	mean: 0.84 SD: 0.06	-
Ratio of 182-day to 28-day Strength	mean: 1.00 SD: 0.04	mean: 1.10 SD: 0.09

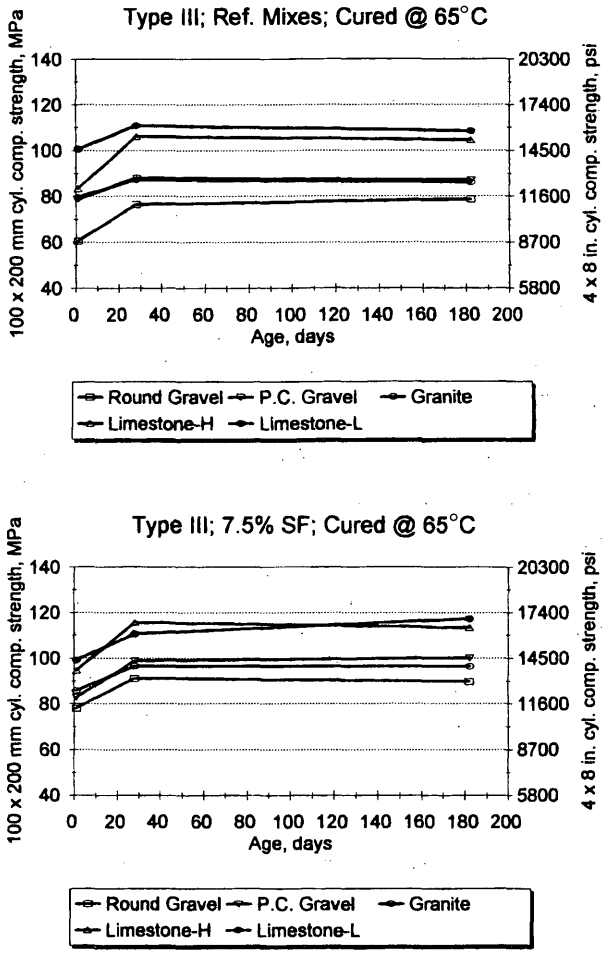

FIGURE 2 Effect of type of aggregate on strength development: reference mixes (*top*) and mixes containing 7.5 percent SF (*bottom*).

RG mixes. The PCG mix failures were attributed to the flaky physical nature of the aggregate. Mineralogical characteristics of the specific granite used were suspected to be the reason for the relatively poor performance of high-strength concrete made with granite.

The difference between the top and bottom of Figure 2 is the cementitious material composition represented (the reference mix versus the 7.5 percent SF replacement by weight of cement mix). The replacement of cement by 7.5 percent SF improved the concrete compressive strength at all ages. In particular, silica fume increased the compressive strength of RG concrete. This can be attributed to the improved bond between the round gravel and the cement paste. More fractured aggregate particles were observed in tests of the RG mix containing silica fume than were observed in the reference mix tests. Moist-curing enhanced the benefit obtained from including silica fume.

Effects of replacement of cement by 20 percent FA, 7.5 percent SF, and the combination of 20 percent FA with 7.5 percent SF on heat-cured high-strength concrete made with GR are shown in Figure 3. For crushed granite, the concrete compressive strength of the 7.5 percent SF mix was highest followed by compressive strengths of the reference concrete and the concrete made with the combination of 20 percent FA with 7.5 percent SF. Concrete mixes containing 20 percent fly ash exhibited the lowest compressive strengths at all ages (to 182 days). The same trend with respect to cementitious material composition was observed for the concretes made with other types of aggregates and curing.

Modulus of Elasticity

The modulus of elasticity was measured after 1 (heat-cured specimens only), 28, and 182 days. Figures 4 and 5 show comparisons of the modulus of elasticity and compressive strengths measured on both 100 × 200 and 150 × 300 mm cylinders relative to equations given in American Concrete Institute (ACI) 318 and proposed by ACI High-Strength Committee 363 (*5,6*). It is clear that for high-strength concrete, the ACI 318 equation overestimates the measured modulus of elasticity of 150 × 300 mm cylinders. Comparing the top and bottom of Figure 5 it is observed that heat-cured specimens exhibited slightly lower moduli of elasticity at any given strength than the moist-cured cylinders.

Of particular interest is the change of modulus of elasticity with time. The initial modulus of elasticity is important to the precast/prestressed industry for investigating effects such as elastic shortening. The later age modulus of elasticity can be used to predict prestress

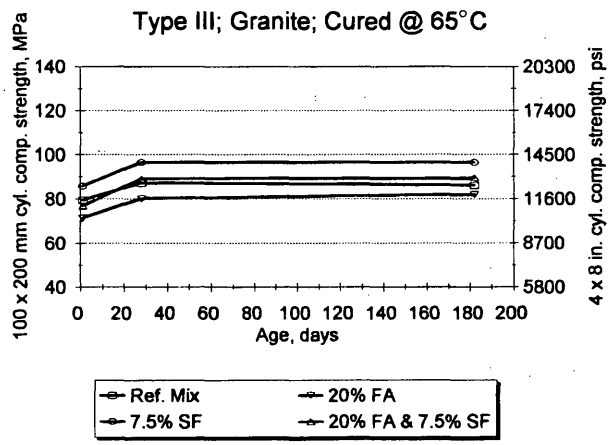

FIGURE 3 Effect of replacement of cement by 20 percent FA and 7.5 percent SF.

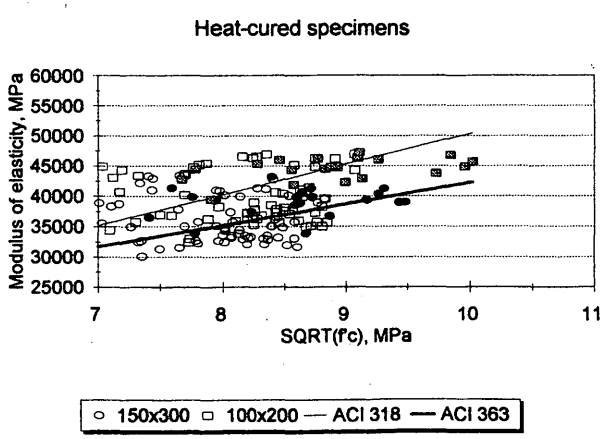

FIGURE 4 1-day modulus of elasticity versus ACI 318 and 363 equations.

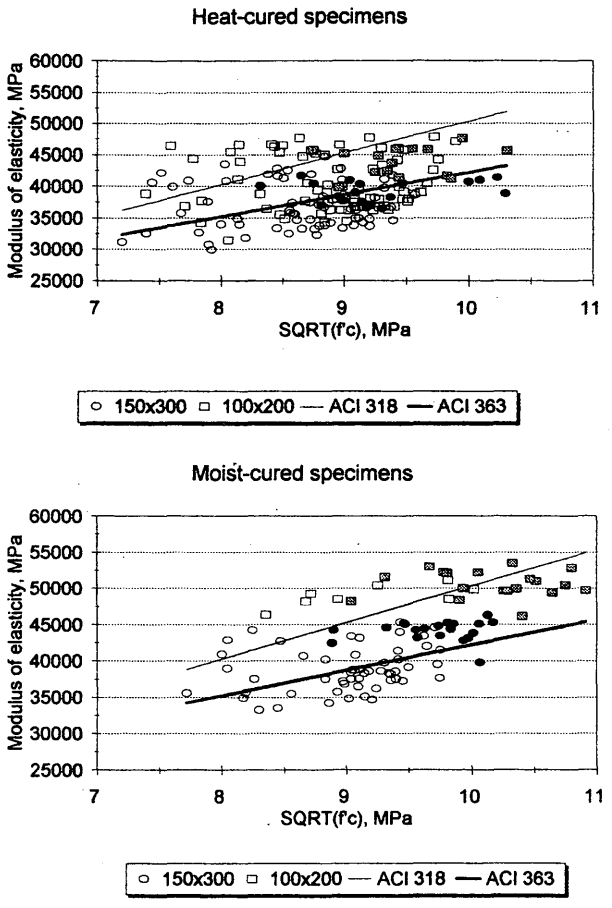

FIGURE 5 28-day modulus of elasticity versus ACI 318 and 363 Equations: heat-cured specimens (*top*) and moist-cured specimens (*bottom*).

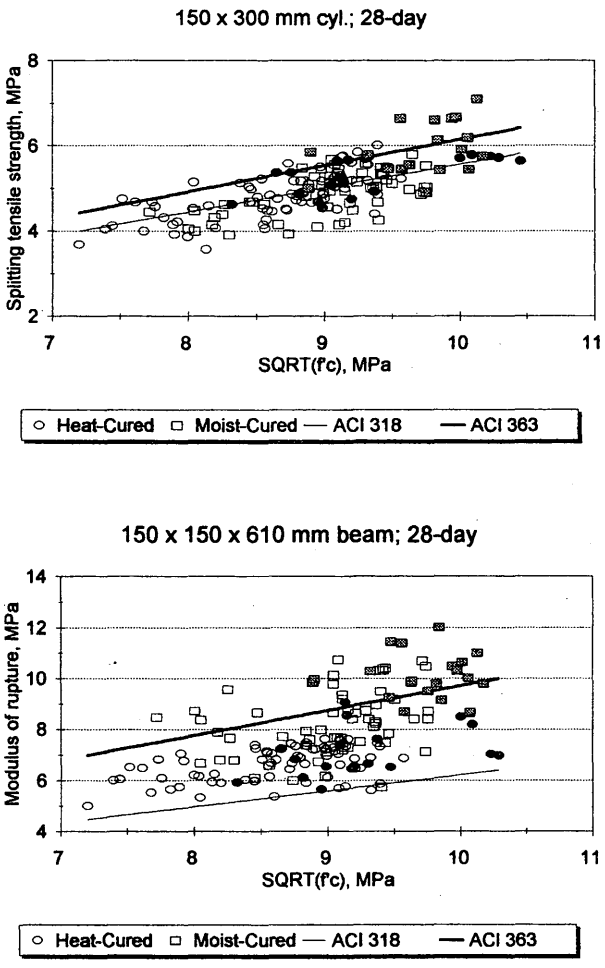

FIGURE 6 Splitting tensile strength test results (*top*) and modulus of rupture test results (*bottom*).

losses and deflection of bridge girders. The results obtained from this study indicate that the 1-day modulus of elasticity measured on heat-cured 100 × 200 mm or 150 × 300 mm cylinders was approximately 98 percent of the 28-day modulus of elasticity value. The modulus of elasticity of the heat- and moist-cured 100 × 200 mm cylinders at 182-days were approximately 96 and 106 percent of their 28-day modulus of elasticity values, respectively.

Tensile Strength

Data obtained for splitting tensile strength of both heat-cured and moist-cured cylinders 150 × 300 mm were more closely predicted by the ACI 318 equation than the proposed ACI 363 relationship. Figure 6 (top) shows results from splitting tensile strength tests conducted on cylinders 150 × 300 mm at 28-days.

Modulus of Rupture

Figure 6 (bottom) shows modulus of rupture test results for heat-cured and moist-cured specimens relative to equations proposed by ACI 318 and ACI 363. Data obtained for modulus of rupture of heat-cured specimens ranged between values predicted by ACI 318 and ACI 363 equations. From this figure, it is evident that the type of curing significantly affected the modulus of rupture test results, with moist-cured samples exhibiting higher flexural strengths. The modulus of rupture of moist-cured specimens was adequately predicted by the ACI 363 proposed equation.

EXPERIMENTAL PROGRAM TO INVESTIGATE FREEZE-THAW DURABILITY

To investigate the durability of high-strength concrete, freeze-thaw studies were conducted on 17 of the mixes in general accordance with ASTM C666 Procedure B (rapid freezing in air and thawing in water). An exception to the standard test procedure was made to investigate the effect of curing on freeze-thaw durability. The standard procedure requires freeze-thaw specimens to be cast and continuously moist cured for 14 days before placing them in the freeze-thaw testing machine. To investigate curing effects, specimens were either heat cured or moist cured for a limited amount of time before being stored in a relatively constant temperature and humidity environment for approximately 6 months. This procedure was intended to simulate casting and aging of cast-in-place and precast/prestressed members before exposing them to freeze-thaw conditions. Other variables investigated were aggregate type and cementitious material composition.

Specimen Preparation and Test Procedure

Four beams 76 × 102 × 406 mm were cast from each mix following ASTM C192 procedures. Manual rodding was used as the method of consolidation. (Measured slumps and air contents are given in Table 2.) As mentioned previously, no air-entraining agents were used to emulate the production of precast/prestressed bridge girders.

Two of the freeze-thaw beam specimens were heat cured, and two were moist cured in a saturated-limewater bath for 7 days. Following the specified curing period, the specimens were placed in an environment of relatively constant temperature and humidity (23°C and 50 percent relative humidity). At 189 days, the specimens were placed in a constant temperature bath at 4.5°C for a period of 21 days before the start of freeze-thaw testing. The 3-week period of immersion was to enable at least partial saturation of the concrete beam specimens before freezing and thawing. This was considered a severe condition because bridge girders are not typically maintained in a saturated moisture condition. Following the 21-day immersion in the constant temperature bath, the first set of concrete beam specimens and some beams from subsequent mixes were placed on a chest freezer and kept at an approximately constant temperature (−18°C) until calibration of the new freeze-thaw testing machine was completed. The calibration was performed in accordance with ASTM C666, which specifies storage of the specimens in a frozen condition if the sequence of freezing and thawing is interrupted. The lengths of time the specimens were kept frozen varied from 0 to 41 days and are provided in Table 4, along with the freeze-thaw test results.

Companion cylindrical specimens 100 × 200 mm were tested to determine absorption potential, which serves as an indirect indicator of concrete permeability (*1*). These specimens were heat cured at 65°C or moist cured for 28 days, as described. After the specified curing period, the specimens were stored in an environment of 23°C and 50 percent relative humidity until they were 56 days old. They were then submerged in water and the weight gain measured with respect to time. This test was still in progress at the time this paper was written; measurements at 105 days are given in Table 4.

Results

The specimens were removed from the freeze-thaw testing machine at intervals conforming to the requirements of ASTM C666; measurements were taken to evaluate deterioration. Changes in specimen weight and length were monitored, and the specimen fundamental transverse frequency was measured in accordance with the ASTM C215, Impact Resonance Method. The relative dynamic modulus (RDM) of elasticity of each specimen was calculated using the fundamental transverse frequency measurements. ASTM C666 requires that the testing of each specimen continue until it has been subjected to 300 freeze-thaw cycles or until it has reached a failure criterion, whichever occurs first. ASTM defines possible failure criteria as the relative dynamic modulus of elasticity reaching 60 percent of the initial modulus or, optionally, a 0.10 percent length expansion. In this study, both failure criteria were considered, and the specimens were removed from the freeze-thaw testing machine when the relative dynamic modulus of elasticity reached 50 percent of the initial modulus.

The average number of cycles after which the failure criteria were met and the corresponding average durability factors (DF) for each pair of specimens are given in Table 4. The number of cycles to observed failure is given for the relative dynamic modulus and the length expansion failure criteria. As can be seen in the table, there is generally a strong correlation between the two failure criteria for all but the limestone aggregate mixes; in which case, the length expansion or dilation criterion was generally reached much more quickly than the relative dynamic modulus criterion. This may be because of the relative inability of the more porous limestone to restrain dilations of the cement mortar when compared with concrete containing the harder gravel and granite aggregates.

The DF for the heat- and moist-cured specimens are plotted in Figure 7 *top* and *bottom*, respectively. The results shown in these figures are grouped according to aggregate type and cementitious material composition.

The following DF scale to evaluate frost-resistant performance was proposed (*7*): concrete with a DF less than 40 is probably unsatisfactory for frost resistance, concrete with a DF between 40 and 60 is of doubtful performance, and concrete with a DF greater than 60 is probably satisfactory for frost resistance. This scale was used to evaluate the effects of curing condition, aggregate type, and cementitious composition. These evaluations follow.

Effect of Curing Condition

Figure 7 *top* and *bottom* indicates that the moist-cured specimens generally exhibited better freeze-thaw durability than the heat-cured specimens. Moist-curing allows continuous hydration of the cementitious materials, developing a less permeable pore structure. The hydration in heat-curing is limited by the amount of mix water. Microcracking could also develop on drying, weakening the strength of the transition zone between the aggregate and the cement paste. These factors result in increased permeability. In the instances in which the heat-cured specimens performed better, the durability factors were less than 25 for the heat- and moist-cured specimens (unsuitable for frost resistance). Both heat- and moist-cured specimens performed satisfactorily (DF > 60) for all LS–L mixes, although moist-curing appeared to provide better durability.

These observations on the effect of curing condition correlate well with the results of the absorption potential tests in which the moist-cured specimens consistently absorbed less water than the heat-cured specimens.

Effect of Aggregate Type

The low-absorption limestone specimens consistently performed the best of all of the mixes (reference, 7.5 percent SF, and combination of 20 percent FA with 7.5 percent SF) for both types of curing, with DFs ranging from 61 to 98. Several of the LS–L specimens endured more than 1,500 freeze-thaw cycles without failing (the RDM criterion) before they were removed from the freeze-thaw testing machine. The moist-cured LS–H and PCG reference mixes also exhibited satisfactory performance. The RG and granite specimens performed the poorest (DF < 15). The order of performance, with the exception of the limestone aggregate specimens, was consistent with the results of the absorption tests. In other words, the limestone specimens exhibited the highest absorption but showed the best performance. Improved performance of the other mixes correlated with reduced absorption.

The good performance of the limestone may be attributed to the surface texture of the aggregate. Angular, rough-surfaced aggregates develop a better bond with the cement mortar, strengthening

TABLE 4 Freeze-Thaw Durability and Absorption Potential Test Results

Mix	Days Frozen Prior to Testing	Cycles to Observed RDM Failure *Length Change Failure*		Durability Factor		Absorption @ 105 days* (% weight)	
		Heat-cured	Moist-cured	Heat-cured	Moist-cured	Heat-cured	Moist-cured
RG	18	34 *34*	80 *80*	5	14	1.27	0.67
RG w/FA	41	26 *30*	85 *85*	5	15	1.62	0.73
RG w/SF	32	34 *34*	26 *30*	6	5	0.78	0.52
RG w/FA&SF	27	48 *41*	26 *26*	7	7	1.10	0.72
PCG	4	71 *62*	1507+(346) *1507+(346)*	12	97	1.20	0.71
PCG w/FA	4	55 *48*	201 *180*	10	40	1.54	0.75
PCG w/SF	0	30 *26*	26 *26*	4	2	0.93	0.61
PCG w/FA&SF	0	68 *58*	35 *38*	12	6	0.87	0.70
GR	0	46 *30*	52 *48*	9	9	1.58	0.78
GR w/FA	0	53 *53*	59 *62*	10	11	1.43	0.82
GR w/SF	0	30 *30*	20 *20*	3	2	0.88	0.59
GR w/FA&SF	0	53 *53*	19 *22*	10	4	1.10	0.69
LS-H	13	469(149) *59*	1507+ *1507(1132)*	66(30)	97	1.59	0.78
LS-H w/FA&SF	6	119 *62*	26 *26*	24	5	1.25	0.98
LS-L	0	1520+ *1520+(1166)*	1520+ *1520+*	96	98	1.35	0.80
LS-L w/SF	0	640 *229*	1510+ *420(240)*	77	81	0.93	0.71
LS-L w/FA&SF	0	308 *161*	1366 *116*	61	71	0.94	0.77

*Test in progress.

+Indicates that the specimens have not yet failed the relative dynamic modulus test.

( ) Indicates value for companion specimen if different.

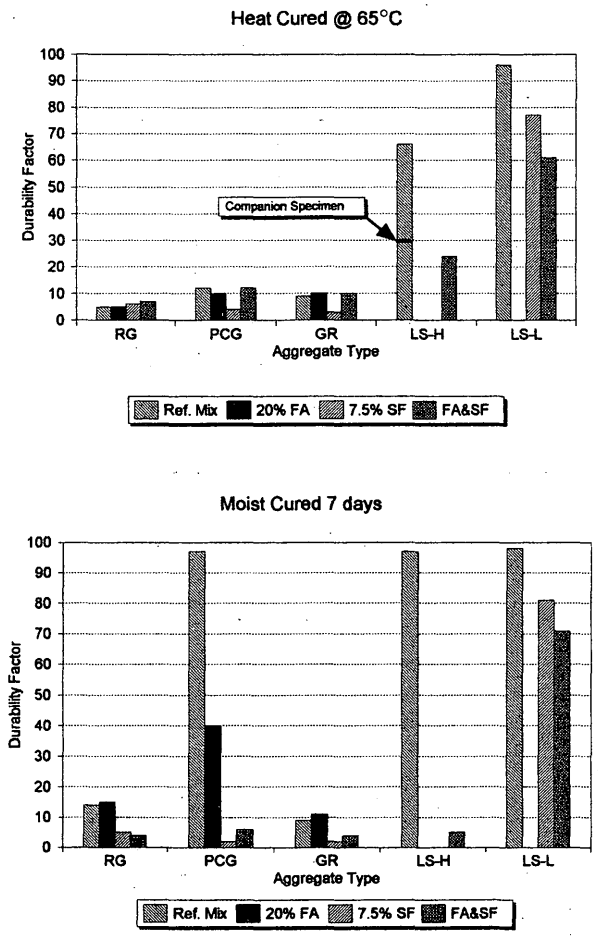

FIGURE 7 Freeze-thaw cycle durability: heat-cured specimens (*top*) and moist-cured specimens (*bottom*).

the transition zone between the paste and aggregate. A weak transition zone could result in microcracking around the aggregates. This theory is supported by the performances of the PGG and RG specimens. When mix composition is held constant, the PCG (with the more angular, rough-surfaced particles) generally exhibited better freeze-thaw durability (see Table 4). For example, the reference concrete mixes made with PCG and RG resulted in durability factors of 12 and 5, respectively.

Although the limestone specimens achieved high durability factors, they generally failed the length expansion test quite early compared with the RDM criterion. The dilation of the limestone mixes that failed the ASTM criteria ranged from 0.20 to 0.38 percent at RDM failure. As previously mentioned, the large dilations observed may be because of the relative inability of the more porous limestone to restrain the expanding cement mortar. The low-absorption limestone reference mix, however, exhibited excellent freeze-thaw durability in terms of both RDM and dilation, withstanding over 1,100 cycles without failing.

Effect of Cementitious Composition

Comparing the results in the *top* and *bottom* of Figure 7, it can be seen that the reference mixes generally performed the best for any given aggregate type. For the moist-cured specimens, the reference mixes prepared using limestone and PCG achieved DFs in excess of 90. The heat-cured limestone reference mixes also generally exhibited satisfactory performance.

For both heat- and moist-cured specimens of the low-absorption limestone, the good performance of the reference mixes was followed by the performances of 7.5 percent SF and the combination of 20 percent FA with 7.5 percent SF mixes. Similar results were seen in the heat- and moist-cured LS–H mixes in which the reference mix exhibited better durability than the 20 percent FA with 7.5 percent SF combination mix.

For the remaining three aggregates (RG, PCG, GR), the effect of variations in cementitious composition strongly correlated with curing condition. All of the heat-cured specimens exhibited poor durability (DF = 3 to 12). When moist-curing was used, the reference and fly ash mixes performed much better than those containing silica fume, especially for the PCG.

The absorption tests have shown that the FA specimens typically absorbed the most water, followed by the reference mix specimens. The SF specimens absorbed the least water, with the silica fume and fly ash with FA combination specimens exhibiting similar performance (with a slightly higher absorption observed for the specimens containing the combination of fly ash with silica fume). There was no apparent correlation between the absorption (indirect permeability measurement) and the durability factor.

Relationship of Compression Strength to Durability

Plots of durability factors versus 28-day compressive strengths of the heat- and moist-cured (7 day) 100 × 200 mm specimens are shown in Figure 8 *top* and *bottom*, respectively. Figure 8 (*top*) appears to show a strong correlation between compressive strength and durability factor for the heat-cured specimens, but on closer examination it can be seen that the relationship is strongly influenced by aggregate type. This is more clearly shown in Figure 8 (*bottom*) for the moist-cured specimens. Data in both figures indicate that for a given aggregate type for which a range of concrete strengths was produced (e.g., for GR, range in f'c of 81 to 120 MPa) little change in durability factor was observed.

The mechanisms that produced the observations and results described will be more fully investigated when analyses of the water pore and air void systems have been completed. This work is now under way.

Ongoing Research

Tests are being performed on the freeze-thaw concrete beams in accordance with ASTM C457 to measure the air void system of the hardened concrete and to determine the mechanism of failure in each case. Additional mixes will be tested to explore reasons for the failures and to identify potential improvements. Additional mixes will also be cast to compare the effects of curing in accordance with ASTM C666 (a 14-day moist cure) with the curing method used in this study. Three mixes are also being repeated to determine the effect, if any, of the period of freezing before testing on the observed durability performance. Two mixes that performed poorly in the study are being remixed with the addition of an air-entraining agent to assess its effect on improving the concrete durability results and to better quantify the durability of the various coarse aggregate sources.

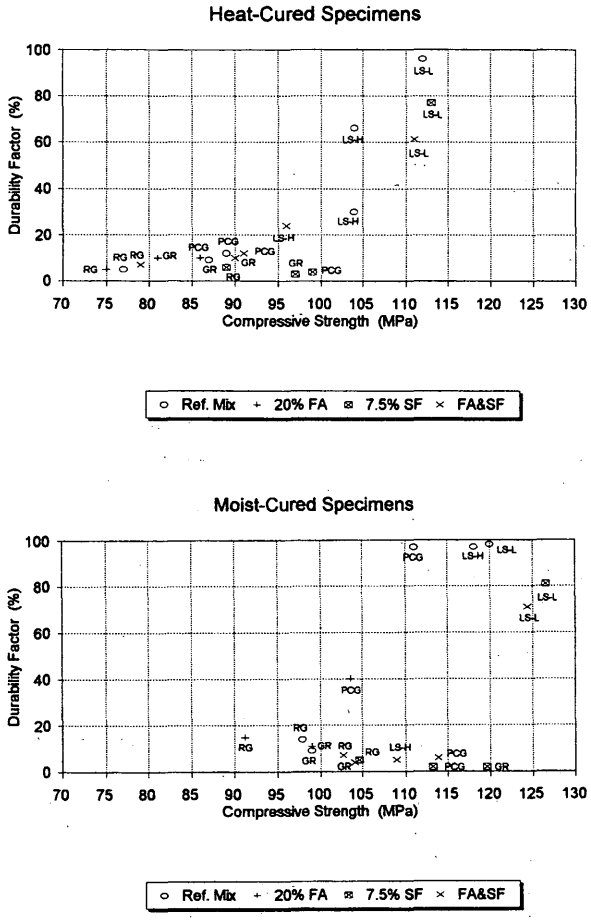

FIGURE 8 Durability factor versus 28-day compressive strength: heat-cured specimens (*top*) and moist-cured specimens (*bottom*).

SUMMARY

Preliminary results of a study of the mechanical characteristics and freeze-thaw durability of high-strength concrete were presented. Over 7,000 specimens have been cast and tested. The results described focus on a portion of the tests in which the total amount of cementitious material, water-to-cementitious material ratio, and coarse-to-fine aggregate ratio was held constant. Variables investigated include cementitious material composition, aggregate type, and curing condition. Results indicate that it is possible to develop non–air-entrained high-strength concrete with superior mechanical properties and freeze-thaw durability characteristics using local aggregate sources. In particular, the limestone reference mixes (without the addition of fly ash and silica fume) offered excellent mechanical and durability characteristics.

ACKNOWLEDGMENTS

This research investigation was conducted under the joint sponsorship of the Minnesota Prestress Association, Minnesota Department of Transportation, University of Minnesota Center for Transportation Studies, Precast/Prestressed Concrete Institute, and National Science Foundation Grant NSF/GER–9023596–02. The authors also acknowledge the generous donations of materials and equipment from Lehigh Cement Company; Holnam, Inc.; National Minerals Corporation; J. L. Shiely Company; Edward Kraemer & Sons, Inc.; Meridian Aggregates; W. R. Grace & Co.; Cormix Construction Chemicals; and Elk River Concrete Products.

REFERENCES

1. Burg, R.G., and B.W. Ost. Engineering Properties of Commercially Available High-Strength Concretes. *PCA Research and Development Bulletin RD104T.* Portland Cement Association, Skokie, Ill., 1992.
2. French, C.W., and A. Mokhtarzadeh. High Strength Concrete: Effects of Curing and Test Procedures on Short Term Compressive Strength. *PCI Journal,* Vol. 38, No. 3, May-June 1993, pp. 76–87.
3. French, C., A. Mokhtarzadeh, T. Ahlborn, and R. Leon. *Applications of High-Performance Concrete to Prestressed Concrete Bridge Girders.* Paper submitted to the International Workshop on Civil Infrastructure Systems, Taipei, Taiwan, Jan. 1994.
4. Minnesota Department of Transportation. *Standard Specifications for Construction,* 1988 ed. St. Paul, Minn. 1988.
5. *Building Code Requirements for Concrete, 318–89* (Rev. 1992). American Concrete Institute, Committee 318, Detroit, Mich., 1992.
6. *State-of-the-Art Report on High-Strength Concrete, 363R–92.* American Concrete Institute, Committee 363, Detroit, Mich., 1992.
7. Neville, A.M. *Properties of Concrete.* Pitman Publishing Ltd., London, England, 1975.

The views expressed herein are those of the authors and do not necessarily reflect the views of the sponsors.

Publication of this paper sponsored by Committee on Performance of Concrete.